Opaline Hydrogels: Polycrystalline Body-Centered-Cubic Bulk Material with an in Situ Variable Lattice Constant

R. Goldberg and H. J. Schöpe*

Institut für Physik, Johannes Gutenberg Universität Mainz, D-55099 Mainz, Germany

Opaline hydrogels were produced as a polycrystalline bulk material with a body-centered-cubic (bcc) structure by immobilization of self-ordered charged colloidal particles crystallized under equilibrium conditions in a poly(acrylamide) matrix. The final size of a polycrystalline sample is about 7 cm³; a single crystal is up to several millimeters in length. The crystal size is tunable by varying the amount of photoinitiator and the hydrogel volume change due to swelling. The resulting photonic crystals are of high quality, showing high-order reflections. These hydrogels show a reversible shift of the diffraction Bragg peak wavelength depending on external conditions due to swelling or shrinking and under applied mechanical stress. The wavelength of the photonic band gap can be shifted over the entire spectrum of visible light ($\Delta\lambda \approx 500$ nm). Bulk material offers the possibility of shifting the position of the main Bragg reflection to smaller and larger wavelengths simultaneously: under compression, the wavelength of the (110) reflection parallel to the direction of compression decreases, while that perpendicular to the direction of compression increases. This observation can only be explained by a uniaxial transformation of the bcc lattice to a body-centered-orthorhombic lattice. Other uniaxial transformations to body-centered-tetragonal, rhombohedral, or triclinic symmetry are possible depending on the direction of compression.

Introduction

Three-dimensional periodic structures built by crystallization of colloidal particles with lattice constants comparable to the wavelength of the visible light act as photonic crystals and can be used as optical filters, antireflective coatings, sensors, and photonic band-gap materials.[1–7]

Under equilibrium conditions, colloidal crystals are formed in suspensions of spherical particles if the particle concentration is higher than the freezing volume fraction of the system used. The colloidal particles either are stabilized by long-range electrostatic repulsion and dispersed in aqueous solvents or are stabilized by sterical stabilization, in which the particles are dispersed in nonaqueous media.[8–10] Because of the long-range nature of the screened Coulombic interaction, colloidal crystals with body-centered-cubic (bcc) structure may form in suspensions of highly charged spherical particles at very low particle concentrations (particle number density $n_p = 10^{17} - 10^{18}$ m⁻³; volume fraction $\varphi = 0.01-0.1\%$) if the concentration c of the screening electrolyte is kept at or below the micromolar level.[11] The pair energy in monodisperse charged colloidal systems can be written on the mean-field level as

$$V(r) = \frac{(Z^*e)^2}{4\pi\epsilon_0\epsilon_r}\left(\frac{\exp(\kappa a)}{1+\kappa a}\right)^2\frac{\exp(-\kappa r)}{r} \tag{1}$$

with the screening parameter κ calculated from the salt concentration c via

$$\kappa^2 = \frac{e^2}{\epsilon_0\epsilon_r k_B T}(nZ^* + n_{salt}) \tag{2}$$

where $\epsilon_0\epsilon_r$ is the dielectric permittivity of the suspension, $k_B T$ is the thermal energy, and $n_{salt} = 2000N_A c$ is the number density of the background electrolyte, with N_A being Avogadro's number. Z^* is the effective charge of the particle and a the particle radius. The interaction is very sensitive to the screening electrolyte, and the crystalline order can be easily destroyed by ionic impurities (increasing n_{salt}).

Out of equilibrium, under the influence of external fields such as confinement and shearing, the position of the phase boundaries, the crystal structure, and the crystal morphology can be modified.[12] In thin cells under low shear rates, the crystals nucleate with their densest packed plane [bcc-(110) and fcc-(111), where fcc = face-centered cubic] at the cell walls. Using this technique, a polycrystalline material of uniformly oriented twin domains can be prepared.[12] At higher shear rates, only hexagonal crystal structures are observed even if the equilibrium structure is bcc. Under confinement and shearing, the fluid crystal phase boundary shifts to

* Corresponding author. E-mail: jschoepe@uni-mainz.de.
(1) A special issue on photonic crystals. *Adv. Mater.* **2001,** *13* (6).
(2) Hayashi, S.; Kumamoto, Y.; Suzuki, T.; Hirai, T. *J. Colloid Interface Sci.* **1991,** *144,* 538.
(3) Imhof, A. In *Nanoscale Materials*; Liz-Marzan, L. M., Kamat, P. V., Eds.; Kluwer Academic: Boston, MA, 2003; pp 423–454.
(4) Lin, S. Y.; Fleming, J. G.; Hetherington, D. L.; Smith, B. K.; Biswas, R.; Ho, K. M.; Sigalas, M. M.; Zubrzycki, W.; Kurtz, S. R.; Bur, J. *Nature* **1998,** *394,* 251.
(5) John, S. *Phys. Rev. Lett.* **1987,** *58,* 2486.
(6) Petrov, E. P.; Bogomolov, V. N.; Kalosha, I. I.; Gaponenko, S. V. *Phys. Rev. Lett.* **1998,** *81,* 77.
(7) Yablonovitch, E. *Phys. Rev. Lett.* **1987,** *58,* 2059.
(8) Okubo, T. *Prog. Polym. Sci.* **1993,** *28,* 481.
(9) Pusey, P. N.; Megen, W. v. *Nature* **1986,** *320,* 340.
(10) Arora, A. K.; Tata, B. V. R. *Ordering and Phase Transitions in Charged Colloids*; VCH: New York, 1996.

(11) Schöpe, H. J.; Decker, T.; Palberg, T. *J. Chem. Phys.* **1998,** *109,* 10068.
(12) Stipp, A.; Biehl, R.; Preis, T.; Liu, J.; Fontecha, A. B.; Schöpe, H. J.; Palberg, T. *J. Physics: Condens. Matter* **2004,** *16,* S3885.

smaller volume fractions or higher salt concentrations compared to the equilibrium one. Further, several additional crystal structures can be observed under strict confinement.[13]

Because of the low particle number density, the elastic modulus of such photonic crystals is quite low (around 1 Pa)[11,14,15] and the crystals can be easily shear-molten by external forces, e.g., small mechanical perturbations. Therefore, it is necessary to fix the position of the particles in a suitable stabilizing matrix. Asher[16,17] was one of the first authors who showed that this is possible by immobilizing particles in a hydrogel polymer matrix. The resulting material can, furthermore, be functionalized by the exchange of the pore solvent and can be used as a chemical sensor. In contrast to closed-packed structures produced by sedimentation of particles or by controlled drying procedures, charged colloidal crystals allow for a change in the lattice spacing and therefore the wavelength of the diffracted Bragg peak by variation of the particle number density. Asher was the first to show that the lattice distance of a hydrogel opal can be changed by the pH and ionic strength. Foulger and co-workers were among the first to show that the interlattice spacing can be tuned by application of external stress.[18,19] In recent publications,[20,21] they propose a uniaxial transformation of the fcc lattice under compression in the [111] direction as a mechanism for explaining the mechanochromic response of the film. In all these studies, thin crystal films with a thickness of around 100 μm ($\sim$300 layers) with fcc, hexagonal-close-packed (hcp), or random hcp (rhcp) structures are presented. Crystal films are prepared at comparatively high volume fractions of about 10% under nonequilibrium conditions using shear flow and confinement and using small sample volumes of about 0.1 mL. The maximum band shift due to swelling and due to compression is about 250 nm.

Other authors[22–29] developed new approaches to stabilize ordered arrays and extended the range of methods, particles, and kinds of matrices. Jethmalani and co-workers[22–24] used

(13) Schöpe, H. J.; Fontecha, A. B.; König, H.; Hueso, J. M.; Biehl, R. *Langmuir* **2006**, *22*, 1828.
(14) Wette, P.; Schöpe, H. J.; Palberg, T. *J. Chem. Phys.* **2002**, *116* (24), 10981.
(15) Schöpe, H. J.; Palberg, T. *J. Colloid Interface Sci.* **2001**, *234*, 149.
(16) Asher, S. A.; Holtz, J.; Liu, L.; Wu, Z. *J. Am. Chem. Soc.* **1994**, *116*, 4997.
(17) Asher, S. A.; Holtz, J.; Weissman, J.; Pan, G. *MRS Bull.* **1998**, *23*, 44.
(18) Foulger, S. H.; Jiang, P.; Lattam, A. C.; Smith, D. W.; Ballato, J. *Langmuir* **2001**, *17*, 6023.
(19) Foulger, S. H.; Jiang, P.; Yiing, Y.; Lattam, A. C.; Smith, D. W.; Ballato, J. *Adv. Mater.* **2001**, *13* (24), 1898.
(20) Foulger, S. H.; Jiang, P.; Lattam, A.; Smith, D. W.; Ballato, J.; Dausch, D. E.; Grego, S.; Stoner, B. R. *Adv. Mater.* **2003**, *15* (9), 685.
(21) Ying, Y.; Xia, J.; Foulger, S. H. *Appl. Phys. Lett.* **2007**, *90*, 071110.
(22) Jethmalani, J. M.; Ford, W. T. *Chem. Mater.* **1996**, *8* (8), 2138.
(23) Jethmalani, J. M.; Ford, W. T.; Beaucage, G. *Langmuir* **1997**, *13* (13), 3338.
(24) Jethmalani, J. M.; Sunkara, H. B.; Ford, W. T.; Willouhgy, S. L.; Ackerson, B. J. *Langmuir* **1997**, *13*, 2633.
(25) Hu, Z.; Huang, G. *Angew. Chem.* **2003**, *115*, 4947.
(26) Iwayama, Y.; Yamanaka, J.; Takiguchi, Y.; Takasaka, M.; Takasaka, I.; Ito, K.; Shinohara, T.; Sawada, T.; Yonese, M. *Langmuir* **2003**, *19* (4), 977.
(27) Kamenetzky, E. A.; Magliocco, L. G.; Panzer, H. P. *Science* **1994**, *263*, 207.
(28) Nakamura, H.; Ishi, M. *Langmuir* **2005**, *21*, 11578.
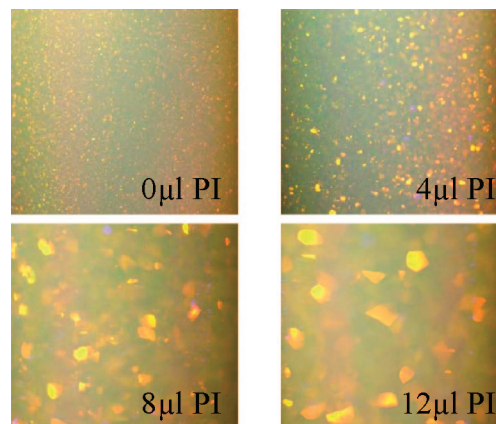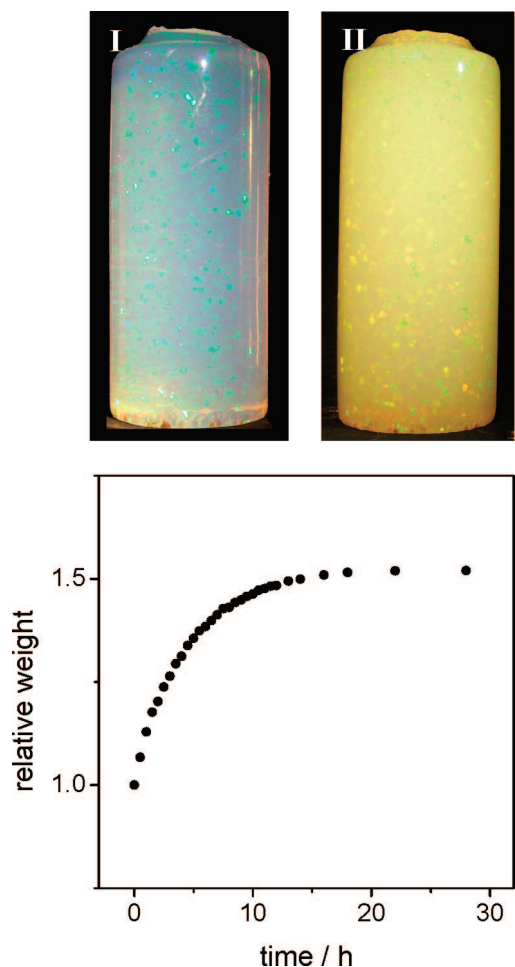(29) Yoshinaga, K.; Fujiwara, K.; Mouri, E.; Idhii, M.; Nakamura, H. *Langmuir* **2005**, *21*, 4471.

Figure 1. Crystal morphology as a function of the added photoinitiator (PI); picture width 1.3 cm. The average crystal size is increasing by addition of the initiator but stays constant in time after the addition. The initiator contains charged molecules right from the start, and so the screening length of the interaction is changed.

surface-modified silica spheres dispersed in MA or MMA. The silica particles form a polycrystalline material with a grain size of $50-200$ μm under equilibrium conditions at volume fractions of around 20%. During polymerization of the MA, the fcc lattice is transformed into a rhombohedral lattice because of anisotropic shrinkage of the crystalline film.

In this work, we present the preparation and characterization of bulk, polycrystalline, bcc gel-stabilized photonic crystals under equilibrium conditions at low volume fractions. We show for the first time a bulk material whose optical response has both a pH dependence and a mechanochromic response to applied stress in both the parallel and perpendicular directions. We produced large samples of polycrystalline bulk material with millimeter-sized randomly oriented crystal grains where the bcc symmetry is maintained. The wavelength of the photonic band gap can be shifted over the entire spectrum of visible light in contrast to previous studies: the hydrogels are optically tunable over a large wavelength interval of more than $\Delta\lambda \approx 400$ nm by changing the pH from 7 to 14 and of more than $\Delta\lambda \approx 500$ nm under applied stress. In addition, the bulk material offers the possibility of shifting the position of the main Bragg reflection to both smaller and larger wavelengths simultaneously as a function of the direction of observation: The wavelength of the band gap parallel to the direction of compression decreases, while that perpendicular to the direction of compression increases. This observation, measured for the first time, can be explained by a uniaxial transformation of the bcc lattice. We show explicitly that the bcc lattice transforms into a body-centered-orthorhombic (bco) lattice by compression in the [110] direction. Other transformations to body-centered-tetrahedral (bct), rhombohedral, or triclinic symmetry are possible as a function of the crystallographic direction of compression.

To produce bulk material, we used negatively charged polystyrene particles with a diameter of 68 nm immobilized in a hydrogel matrix. These particles have been thoroughly characterized by various methods previously, and it was confirmed by static light scattering experiments that these particles crystallize in a lattice with bcc symmetry under salt-free conditions.[14] To immobilize the particles in a cross-

Figure 2. Top: Opaline hydrogel before (I; 3.75 × 1.55 cm, weight 8.2 g) and after swelling (II; 4.53 × 1.90 cm, weight 12.4 g) in water. Pictures were taken under white-light illumination and show a Bragg peak shift from blue-green to yellow with increasing lattice spacing. Bottom: Relative mass increase during swelling in water (pH = 7) as a function of time.

linked polymer matrix, we adopted a procedure similar to Asher's method of photoinitiated free-radical polymerization.

Experimental Section

Negatively charged colloidal polystyrene particles (PnBAPS68, a copolymer of *n*-butylacrylamide, lot no. ZK2168/7387, a kind gift of BASF, Ludwigshafen, Germany) with a diameter of $2a = (68 \pm 3)$ nm measured by ultracentrifugation and electrostatically stabilized by sulfate groups (charge number $N = 1435$ from titration; effective charge $Z^*_G = 331 \pm 3$ from crystal elasticity) suspended in water were used to prepare the suspension. The stock solution with a particle number density of $n_p = 2.1 \times 10^{21}$ m^{-3} was diluted with water purified by an Elga Laboratory Water system. The monomer and cross-linker must be water-soluble, and therefore we used acrylamide and as the cross-linker *N,N'*-methylenebis(acrylamide) (Merck) both in powder form as received without further treatment and purification. To prepare aqueous monomer–cross-linker solutions, the reactants were dissolved in purified water under continuous of stirring at a mass ratio of 15:1 and concentrations of 4.7 mol/L monomer and 0.15 mol/L cross-linker. The colloidal dispersion was mixed with the monomer–cross-linker solution and deionized by use of mixed-bed ion-exchange resin beads (Amberlite, Roth GmbH) until homogeneous crystallization (indicated by the appearance of blue-green diffraction spots) occurred throughout the solution. The mixture had a final particle number density of $n_p =$

1.2×10^{20} m^{-3} ($\varphi = 2\%$) and was stable in closed vessels for several days. Then self-polymerization of acrylamide started, and melting of the crystals was observed. To avoid contact with CO_2 from air (ionic impurities), the sample solution was transferred directly into vials under an argon atmosphere and mixed with an UV-light-curable photoinitiator (2,2-diethoxyacetophenone, DEAP; Sigma Aldrich). To cure the monomer and to polymerize the gel, the recrystallized sample was then illuminated by use of an UV-light lamp (Leica/LEITZ Hg 50 W) for several minutes. Cylindrical samples with volumes of up to 7 cm^3 could be produced. In closed containers, the samples are long-time stable, at least over 3 years. However, continuous exposure to air resulted in dehydration of the samples. This led at first to a blue shift of the opalescence until no color was visible and the gel was irreversibly hardened. The resulting hydrogel consists of anearly 60% hydrophilic polymer network. After removal of the samples from the vials, they were swollen in water or in highly alkaline solutions (NaOH, pH = 14) until equilibrium (there was no further mass change) was achieved. To observe the optical behavior of the swollen samples under applied mechanical stress, a special sample holder (Figure 4) equipped with a micrometer head connected to a fiber spectrometer (Avantes AvaSpec-2048) was used. This holder was mounted in the center of a homemade goniometer. Inside the holder, the sample was standing on a glass plate of 1 mm thickness, and a spherical plate made of stainless steel was driven by the micrometer head compressing the sample. To determine the lattice constant parallel to the direction of compression, the backscattering probe of the spectrometer was connected from below. To measure the lattice constant perpendicular to the direction of compression, the back-scattering probe of the spectrometer was mounted on the goniometer arm.

Results and Discussion

Among several experimental parameters, the amount and concentration of the photoinitiator (DEAP) has the most significant effect on the system and influences the initial crystal size. The radical-containing initiator has the same effect as the addition of salt and changes the absolute value and the range of the interaction by varying the screening length. With increasing volumes of the initiator, the crystal size is increasing, as shown in Figure 1. This is in good agreement with previous studies changing the interaction by varying the particle concentration and/or salt concentration.[30,31] Higher concentrations of the initiator lead to melting of the crystals.

The swelling behavior of our opaline hydrogels in ultrapure water is shown in Figure 2. A free-standing cylindrical sample of a polymerized polycrystalline colloidal crystal prepared by the described method is shown before and after swelling to equilibrium for 30 h in water. The sample dimensions changed from 3.75 × 1.55 cm, weight 8.2 g, to 4.53 × 1.90 cm, weight 12.4 g. This is comparable to a mass change of 50% and an isotropic volume change of 80%, as shown in Figure 2. Both samples show colors caused by Bragg diffraction. Because of the increase of the lattice constant during swelling, the Bragg back-reflection color changes from blue-green to yellow.

(30) Okubo, T. *Langmuir* **1994**, *10*, 1695.
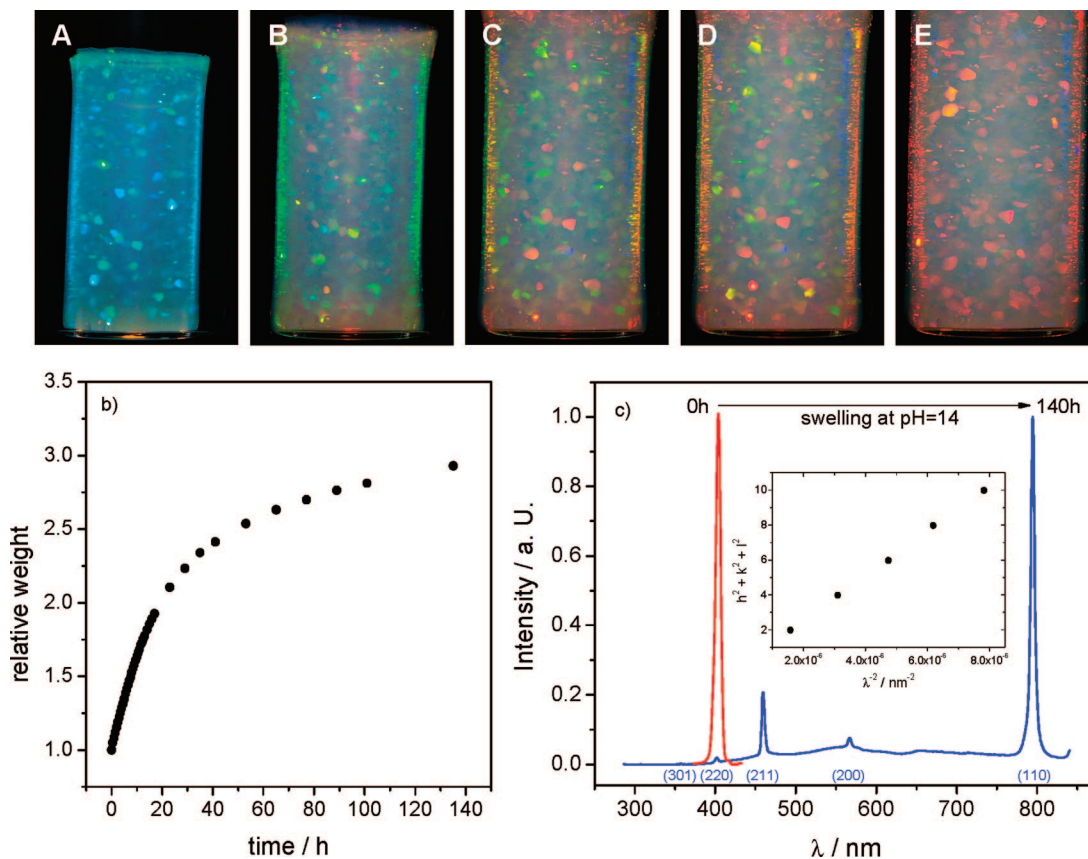(31) Wette, P.; Schöpe, H. J. *Phys. Rev. E* **2007**, *75*, 051405.

Figure 3. (Top) Swelling of a hydrogel after different periods of time: (A) $t = 0$ h; (B) $t = 5$ h; (C) $t = 17.5$ h; (D) $t = 23.5$ h; (E) $t = 100$ h in a NaOH solution (pH = 14); picture width 2.5 cm. (Bottom left) Swelling behavior of an opaline hydrogel in NaOH (pH = 14) as a function of time. (Bottom right) Reflection spectra of the sample shown on top at $t = 0$ and 140 h. The peak position of the bcc-(110) peak shifts about $\Delta\lambda = 400$ nm during the swelling process. During swelling, the bcc structure is maintained, as shown in the inset.
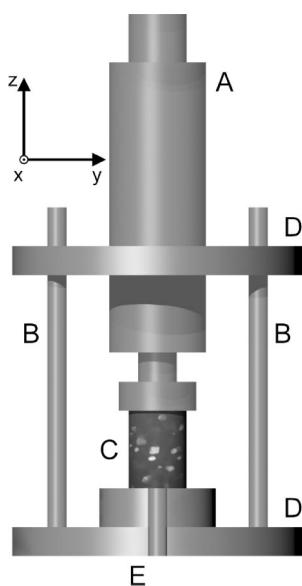

Figure 4. Schematic view of the sample holder used to compress the hydrogel in the z direction: A, micrometer head; B, guide screws; C, polycrystalline hydrogel sample; D, polycarbonate plates; E, fiber connection to the spectrometer.

The extent of swelling is more pronounced in alkaline solutions, as shown in Figure 3 for different periods of time in a NaOH solution with pH = 14. The sample dimensions change isotropically from 1.27×3.1 cm, $m = 4.37$ g at $t = 0$, to 1.71×4.29 cm, $m = 13.11$ g at $t = 6$ days. This is comparable to a volume and mass change of about 200%. In contrast to the water-swollen sample, the Bragg reflection color shifts to a more extended range and changes from blue-green to purple. The wavelength of the observed Bragg reflection is described by Bragg's law, which simply reads as follows:

$$\lambda_{hkl} = \frac{2g\nu_{sample}}{\sqrt{h^2 + k^2 + l^2}} \sin\left(\frac{\Theta}{2}\right) \qquad (3)$$

where λ_{hkl} is the observed wavelength of the peak, h, k, and l are the Miller indices, Θ is the scattering angle, g is the lattice constant, and ν_{sample} is the refractive index of the sample given by $\nu_S = [\Phi\nu_P^2 + (1 - \Phi)\nu_M^2]^{1/2}$. Here φ is the packing or volume fraction of the crystal, and ν_P is the refractive index of the particles dispersed in a medium of refractive index ν_M. Figure 3c shows the shift of the bcc-(110) reflection measured by reflection spectroscopy (scattering angle of 180°) shifting from 400 to 795 nm, covering the whole spectra of visible light. Also, after swelling, a high-quality bcc structure is maintained, as can be seen from the higher order reflection and the inset in Figure 3c. Using a deuterium lamp instead of a halogen lamp, the intensity of the spectrum at low wavelength is increased, which gave us the possibility of identifying high-order peaks in the un-swollen state. This is not shown in Figure 3c for clarity. The (200) peak can clearly be identified at a wavelength of 283 nm [(110) peak at 404 nm]. The swelling behavior in water and NaOH solutions is reversible.

To study the optical behavior of the hydrogels under applied uniaxial mechanical stress, a part of the gel was set between two parallel plates and compressed in the z direction by use of a micrometer head to a certain thickness (Figure 4). Here nonswollen, partly swollen, and swollen gels have been used. The reflection spectra were measured first in the x direction and then in the z direction. The maximum decrease in the relative length before destruction of the samples was $\Delta l/l \approx 60\%$. Because of the increase of the lattice spacing in the xy direction, a continuous red shift of the (110) Bragg peak is observed, whereas in the z direction, the lattice constant decreases and therefore a blue shift is obtained (Figure 5). After the sample is released from compression, the elastic polymer network returns immediately to its initial shape and diffraction color.

The observation that the position of the (110) Bragg reflection parallel and perpendicular to the direction of the applied stress shifts simultaneously to smaller and larger wavelengths can be impressively demonstrated by compressing a partly swollen sample. Here the equilibrium Bragg reflection is green and, upon compression, changes to red in the xy direction and blue in the z direction. Figure 5a shows three photographs of the sample during compression. The shift of the (110) reflection to larger wavelength in the xy direction (perpendicular to the direction of compression) is clearly visible. The quantitative measurement is shown in Figure 5b. It is observed that the wavelength of the (110) reflection in the xy plane is constant by rotation of the reflection probe around the z axis. The position of the peak shifts by about 224 nm from 546 to 770 nm, covering about 50% of the visible spectrum. A linear relationship between the wavelength shift and the change of the relative length of the sample is observed (Figure 5d). As can be seen in Figure 5c, the (110) peak shifts to smaller wavelength in the z direction (parallel to the direction of compression). Again a linear relationship between the wavelength shift and the change of the relative length is observed. Here the position of the peak shifts by about 246 nm from 546 to 300 nm, covering about 50% of the visible spectrum. According to Bragg's law, the lattice constant increases in the xy direction from 290.3 to 409.4 nm (41%) and decreases in the z direction from 290.3 to 159.5 nm (45%). The ratio of the relative change in the lattice constant parallel and perpendicular to the applied stress, $\Delta g_{xy}(\Delta z)/\Delta g_z(\Delta z) = 0.6$ (Figure 5c), is in good agreement with the Poisson ratio μ of the hydrogel, which was determined to be 0.57 by measuring the change of the sample diameter as a function of the compressed sample height. The sample diameter changes isotropically under compression.

The origin for these observations is a uniaxial transformation of the original bcc crystal. In principle, there are two possible transformations under compression in the z direction: The variation of the interparticle distance in the xy plane is isotropic ($\Delta d_x = \Delta d_y$) or anisotropic ($\Delta d_x \neq \Delta d_y$). The change of the particle positions inside the lattice under compression is a function of the mechanical response of the hydrogel. Under compression in the z direction, it is observed that the expansion of the hydrogel in the xy plane is isotropic. Further we observe that the
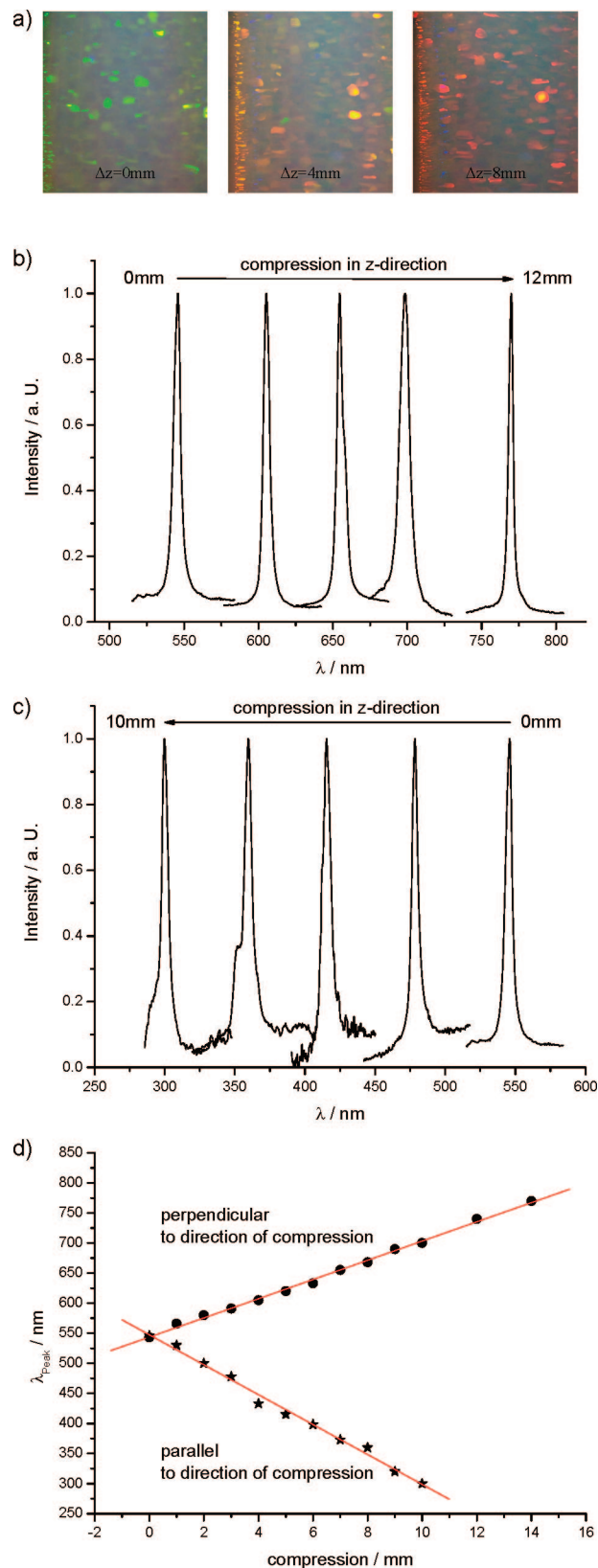

Figure 5. (a) Hydrogel sample under mechanical stress; picture width 1.4 cm. With increasing compression Δz, a reversible green to red shift can be observed in the x direction. Reflection spectra of the swollen hydrogel showing the (110) peak during compression in the z direction: (b) red shift observed in the x direction ($\Delta\lambda = 250$ nm; $\Delta z = 14$ mm); (c) blue shift observed in the z direction ($\Delta\lambda = 250$ nm; $\Delta z = 10$ mm). (d) The obtained wavelength shift is linear with compression.

wavelength of the (110) reflection in the xy plane is constant by rotation of the sample around the z axis.
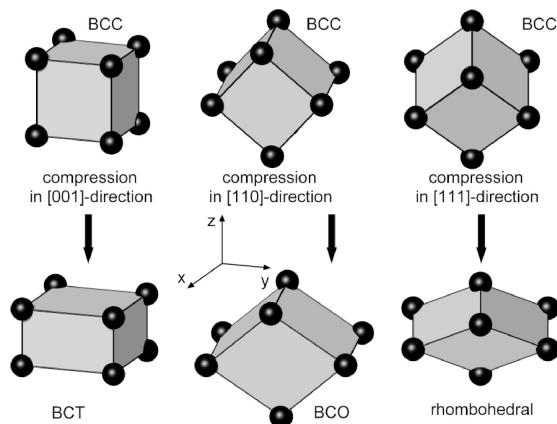
Figure 6. Hydrogel with immobilized colloidal particles under applied mechanical stress in the *z* direction. The interparticle distance in the *z* direction decreases, while it increases in the *xy* plane. From left to right: Under compression in the [100] direction, the crystal symmetry changes from cubic bcc (point group *Im*$\bar{3}$*m* to bct (point group *I*4*mm*), under compression in the [110] direction to bco (point group *Immm*), and under compression in the [111] direction to bct, which is not a Bravais lattice and can therefore be indexed as a half-sized rhombohedral (point group *R*$\bar{3}$).

The uniaxial transformation of the bcc lattice depends on the direction of compression. In the experiment, we measured the compression of crystals in the [110] direction. Because the variation of the interparticle distance in the *xy* plane is isotropic, the bcc lattice converts into a bco lattice, as shown in Figure 6 in the middle. In a polycrystalline material, all crystal orientations are present, and under different orientations, different transformations are possible. Figure 6 shows two additional possibilities: by compression of the bcc crystal in the [100] direction (Figure 6, left), the lattice transforms into a bct lattice, compressing in the [111] direction (Figure 6, right) into a rhombohedral lattice. By compression of the crystal in any other direction, the bcc lattice transforms into a triclinic lattice.

Summary

The preparation of polycrystalline bulk gel-stabilized photonic crystals with a bcc structure has been presented. Samples with large volumes and domain sizes of up to several millimeters in length can be prepared. The crystal size can be tuned via the amount of the added photostarter and the swelling procedure. The crystalline order of bcc symmetry is maintained after polymerization, but the matrix of the gel is soft and flexible and therefore the interparticle distance can be reversibly changed by swelling/shrinking or by applied mechanical stress. During swelling in an alkaline solution, the Bragg peak shift covers the complete range of visible light from blue to red. Also under compression, the color of the Bragg reflection is tunable over a range of more than 500 nm. The equilibrium position of the noncompressed sample can be adjusted by the swelling procedure or by variation of the initial particle number density. By compression of the photonic crystal, the interparticle distance parallel to the direction of compression increases, while perpendicular to it, the interparticle distance increases. The use of a bulk material offers the possibility of using both effects simultaneously. The observed shift of the Bragg peak parallel and perpendicular to the direction of compression can be explained with a uniaxial transformation of the bcc crystal. The structure after compression is a function the lattice orientation in the sample. We verified the transformation of a bcc lattice into a bco lattice if the (110) planes are oriented perpendicular to the direction of compression. We propose transformations into bct, rhombohedral, and triclinic structures as a function of the crystal orientation.